RAPID COMMUNICATION

Serum MEPE-ASARM-peptides are elevated in X-linked rickets (HYP): implications for phosphaturia and rickets

Doron Bresler[1,5], Jan Bruder[2], Klaus Mohnike[3], William D Fraser[4] and Peter S N Rowe[5]

[1]United States Air Force (USAF) Lackland, San Antonio, Texas, USA

[2]University of Texas Health Science Center at San Antonio, Dept of Medicine, Floyd Curl Drive, San Antonio, Texas 78229, USA

[3]Otto-von-Guericke Universität, Magdeburg, Zentrum f. Kinderheilkunde, Germany

[4]University of Liverpool, Department of Clinical Chemistry, Royal Liverpool University Hospital, Liverpool, United Kingdom

[5]University of Texas Health Science Center at San Antonio, Dept of Periodontics, Floyd Curl Drive, San Antonio, Texas, 78229, USA

(Requests for offprints should be addressed to P S N Rowe; Email: rowep@uthscsa.edu)

Abstract

MEPE (Matrix Extracellular PhosphoglycoprotEin) expression is markedly elevated in X-linked-hypophosphatemic-rickets (HYP) and tumor-induced osteomalacia (TIO). In normal individuals, circulating serum-levels of MEPE are tightly correlated with serum-phosphorus, parathyroid hormone (PTH) and bone mineral density (BMD). Also, MEPE derived, C-terminal ASARM-peptides are candidate minhibins and/or phosphatonins. Our aims were to determine: 1. whether MEPE-ASARM-peptide(s) are abnormally elevated in HYP/hyp serum, and, 2. whether the ASARM-peptide(s) accumulate in hyp mice kidney renal-tubules. Using a specific competitive ELISA we measured a five fold increase ($P=0{\cdot}007$) of serum ASARM-peptide(s) in human HYP patients (normal subjects 3·25 μM n=9; S.E.M.=0·51 and HYP-patients 15·74 μM, n=9; S.E.M.=3·32). A 6·23 fold increase ($P=0{\cdot}008$) was measured in hyp male mice compared with their normal male siblings (normal-siblings, 3·73 μM, S.E.M.=0·57, n=3; and hyp-mice 23·4 μM, n=3, S.E.M.=4·01). Renal immuno-histological screening also revealed a dramatic increase of ASARM-peptides in regions anatomically consistent with the proximal convoluted tubules. This study demonstrates for the first time that markedly elevated serum levels of protease-resistant ASARM-peptide(s) occur in HYP/hyp and they accumulate in murine hyp kidneys. These peptides are thus likely responsible for the phosphaturia and defective mineralization in HYP/hyp and TIO.

Journal of Endocrinology (2004) **183,** R1–R9

Introduction

Defects in the PHEX gene (a Zn-metallopeptidase) are primarily responsible for familial X-linked hypophosphatemic rickets (HYP) (HYP-consortium *et al.* 1995). The clinical and biochemical features of the disease have been described in detail (Drezner 1990, Drezner 2003, Quarles & Drezner 2001, Rowe 1998, Rowe 2004). The key features include hypophosphatemia, inappropriately reduced serum 1,25-vitamin D3, defective mineralization (rickets/osteomalacia) and intrinsic osteoblast defects. The defects in the mouse hyp osteoblast are mediated by a low molecular-weight protease-resistant factor and a similar factor is secreted by TIO tumors (Cai *et al.* 1994, Jonsson *et al.* 2001, Lajeunesse *et al.* 1996, Nelson *et al.* 2001, Nelson *et al.* 1996, Nelson *et al.* 1997, Nesbitt *et al.* 1999, Rowe *et al.* 2000, Wilkins *et al.* 1995, Xiao *et al.* 1998). This factor is specifically released by primary hyp mouse osteoblast cultures and inhibits mineralization and renal phosphate uptake (Lajeunesse *et al.* 1996, Nesbitt *et al.* 1999, Xiao *et al.* 1998). MEPE, a matrix extracellular phosphoglycoprotein was recently cloned from a tumor resected from a patient with TIO (Rowe *et al.* 2000), a disease with striking similarities to familial HYP. MEPE is highly expressed in osteoblasts, osteocytes and the expression is temporally coordinated with PHEX (Argiro *et al.* 2001, Bai *et al.* 2002, Gowen *et al.* 2003, Guo *et al.* 2002, Nampei *et al.* 2004, Petersen *et al.* 2000, Rowe *et al.* 2000, Siggelkow *et al.* 2004). MEPE expression is not only elevated in TIO tumors but is also strikingly elevated in primary osteoblasts derived from hyp mice (murine homologue of X-linked rickets) (Argiro *et al.* 2001, Bai *et al.* 2002, De Beur *et al.* 2002, Guo *et al.* 2002, Liu *et al.* 2003, Rowe 2004, Rowe *et al.* 2000,

Journal of Endocrinology (2004) **183,** R1–R9, Accepted 15 October 2004
0022–0795/04/0183–R1
DOI: 10.1677/joe.1.05989
Online version via http://www.endocrinology-journals.org

Seufert *et al.* 2001, Shimada *et al.* 2001). MEPE has also been shown to be phosphaturic *in vivo* and *in vitro* and inhibits mineralization *in vitro* (Dobbie *et al.* 2003, Rowe *et al.* 2004*b*). The levels of MEPE in normal serum (476 +/- 247 ng/ml) are tightly correlated with serum PO_4, PTH and bone mineral density (Jain *et al.* 2004). MEPE expression is also suppressed by 1,25 vitamin D3 (Argiro *et al.* 2001). Direct administration of recombinant MEPE increases 1,25 vitamin D3 serum levels (Rowe *et al.* 2004*b*) and vitamin D receptor null-mutants (VDRKO) have increased expression of MEPE (Okano *et al.* 2003, Rowe *et al.* 2004*b*). Moreover, MEPE expression is tightly correlated with FGF-23 expression a known mediator of changes in vitamin D metabolism, mineralization and renal phosphate handling (Liu *et al.* 2003).

This combination of biochemical and physiological features suggests that MEPE and/or MEPE processed peptides play major roles in the pathophysiology of HYP and TIO. Further support for this hypothesis is the finding that PHEX protects MEPE from proteolysis *in vitro* (Guo *et al.* 2002). Moreover, using surface-plasmon-resonance (SPR) technology, we have also shown that MEPE forms a specific, Zn-dependent protein–protein interaction with PHEX via the MEPE C-terminal ASARM-motif (Rowe *et al.* 2004*a*). We have proposed that the well documented elevated protease levels in hyp and loss of sequestration by mutated PHEX will result in an increase in protease-resistant free ASARM-peptide levels (Rowe 2004, Rowe *et al.* 2004*a*, Rowe *et al.* 2004*b*). The elevated serum ASARM-peptide levels in turn will inhibit mineralization and renal phosphate handling.

Thus, the evidence clearly supports the potential pathophysiological role of the free ASARM-peptide in HYP and TIO. However, it is not known whether the relative serum levels of ASARM-peptide(s) are actually elevated in these diseases. In this paper, we present evidence for the first time that confirms markedly elevated serum ASARM-peptide in humans and mice affected with X-linked hypophosphatemic rickets. Moreover, the levels are entirely commensurate with the amounts of peptide required to seriously impact mineralization and renal phosphate handling (Rowe *et al.* 2004*a*, Rowe *et al.* 2004*b*). Also, renal immunological staining of hyp mice kidneys show an unequivocal increase in ASARM-epitope staining of anatomical structures consistent with the proximal convoluted tubules in hyp mice relative to normal littermates. These new findings will hopefully be of use for the design of new regimes for the clinical management of HYP, TIO, renal disease and diverse bone-mineral loss disorders.

Materials and Methods

Serum samples

Serum from families with X-linked hypophosphatemic rickets (HYP), from affected and non-affected individuals were previously described and obtained under approved IRB protocols (HYP-consortium *et al.* 1995, Rowe *et al.* 1994, Rowe *et al.* 1996, Rowe *et al.* 1997). All clinically affected members had fully characterized mutations in the PHEX gene and as previously described were part of a data-set originally used to map and clone the HYP gene. Sera from nine affected HYP patients (three affected males (hemizygous), and six females) and nine normal subjects (five male and four females) were analyzed. Hyp mice were purchased from the JAX laboratories (Bar Harbor, ME, USA) with the mutation bred into a C57/BL6 background. Standard PCR and southern genotyping was used to confirm hyp phenotypes (Strom *et al.* 1997). The sera from six male hyp mice, three affected (hemizygous) and three normal individuals were used in this study.

MEPE-ASARM-peptide (phosphorylated and non-phosphorylated) and polyclonal antibodies

The carboxy terminal region of MEPE containing residues 507–525 were synthesized using routine techniques by multiple peptide cloning systems (Multiple Peptide Systems, San Diego, CA). For ELISA studies, both phosphorylated and non-phosphorylated peptides were synthesized. The phosphorylated form of the peptide (NH_2-RDDSSESSDSG(Sp)S(Sp)E(Sp)DGD-COOH) was biotinylated using a Pierce EZ-Link Sulfo-NHS-LC-Biotinylation Kit and the peptide de-salted using an Amersham Biosciences PD-10 desalting column. Both phosphorylated and non-phosphorylated peptides were equally effective in competition assays and the non-phosphorylated form was routinely used to generate standard curves (see Fig. 1A and B). Rabbit polyclonal antibodies raised against ASARM-peptide NH_2-CFSS RRRDDSSESSDSGSSSESDGD-COOH were used in these studies and have been previously described (Rowe *et al.* 2004*b*). Pre-immune sera from the same rabbits were used as negative controls.

ELISA assay

A new enzyme-linked-immunosorbent-assay (ELISA) was designed to specifically quantitate ASARM-peptide(s) in sera from humans and mice. The important components of this assay included 96 well Reacti-Bind Protein-G Coated Plates (Pierce& Co), anti-ASARM-peptide polyclonal antibody (see above), non-phosphorylated ASARM-peptide (also described above), a biotinylated ASARM-peptide (bio-ASARM-peptide), streptavidin horseradish-peroxidase conjugate (Zymed Laboratories, Inc., South San Francisco, CA), and an ECL Advance chemiluminescent detection kit (Amersham BioSciences, Piscataway, NJ). The overall rationale behind the ELISA was briefly as follows. Initially, the Protein-G-immobilized 96 well plates were used to specifically bind anti-ASARM-IgG antibodies. Synthetic bio-ASARM-peptide

was then bound specifically to the immobilized ASARM-antibodies and streptavidin conjugated to horseradish-peroxidase was then allowed to bind to the biotin of the bio-ASARM-peptide. The highly sensitive ECL reagent light-emission system (Amersham Biosciences) was then used to generate a horseradish-peroxidase catalyzed light-signal. The light-signal was in turn detected by a highly sensitive BioRad FluorImaging system camera (− 40 °C, peltier-cooled, 1340 × 1040 pixel CCD resolution, CCD digital-camera). Quantitation of chemiluminescence was carried out using Quantity-1, Bio-Rad, imaging-software. Pixel saturation was prevented by internal software-calibration and exposure adjustment. All light-emission readings were thus accurately quantitative and non-saturating. Pre-incubation of bio-ASARM-peptide with increasing amounts of synthetic non-biotinylated ASARM-peptide prior to addition to plates coated with protein-G-anti-ASARM antibody resulted in a peptide competition for binding to the immobilized anti-ASARM-peptide polyclonal IgG. This in turn resulted in a quenching of the chemiluminescent signal as a function of increasing amounts of non-biotinylated ASARM-peptide in the presence of a constant amount of bio-ASARM-peptide. Maximum chemiluminescence (0% quenching) was achieved in the absence of non-biotinylated peptide (full bio-ASARM-peptide mediated light-signal emission) and maximum quenching (100%) was achieved in the presence of excess non-biotinylated ASARM-peptide (reduced light emission and binding of bio-ASARM-peptide). Pre-immune serum was also used as a negative control (zero chemiluminescence). Thus, maximum light or 0% quenching indicates low levels of standard synthetic ASARM-peptide or ASARM-peptides in the experimental unknown, and, low-light emission or maximum quenching (100%) is indicative of high concentrations of ASARM-peptide. The following describes the experimental protocol in more detail.

First, to block non-specific binding, 40 µl of Tris–buffered saline (TBS) supplemented with 0·1% (v/v) Tween-20, and 5% non fat dried skimmed milk (TBST-M; Amersham-Biosciences CAT No: RPN2125V) was added to each well of 96 well Protein G coated plates and then incubated at 5 °C with shaking overnight. Plates were then washed three times with the same buffer but without the non-fat dried skimmed milk (TBST). After washing with TBST, 40 µl of a 1:4000 dilution of anti-ASARM antibody was added to each well (diluted in TBST-M). Plates were then incubated at room temperature for 1 h to facilitate binding of anti-ASARM IgG antibodies to plate-immobilized protein-G. Plates were then washed three times with a TBST. The competition assay was then carried out by separately mixing a constant 0·5 ng/ml concentration of bio-ASARM-peptide with differing concentrations of non-biotinylated ASARM-peptide standards (standard curve) or a range of dilutions of sera as discussed in results and shown in Fig. 1A and B. All dilutions were made using the TBST buffer. For competition with a 0·5 ng/ml bio-ASARM-peptide the following standard concentrations of non-biotinylated ASARM were optimal: 250, 187, 125, 93, 60, 30, 15 and 7·5 ng/ml (Fig. 1). Both pre-immune sera and excess non-biotinylated ASARM (1 µg/ml) were used as separate negative controls (zero chemiluminescence). The competition solutions (40 µl) were then added to individual wells of the 96 well plate containing immobilized anti-ASARM-IgG and left for 1 h at room temperature. Plates were than washed three times with TBST solution. Forty micro-liters of a 1:20 000 dilution of streptavidin horseradish peroxidase conjugate in TBST was then added to each well and incubated for 25 min at room temperature. The plate was washed a further three times with TBST and then directly developed with ECL plus-Advance chemiluminescence kit reagents (Amersham Bioscience). The plate was then left to incubate for 5 min in the dark and reagents removed from each well prior to chemiluminescence detection by the FluorIamger camera (BioRad). Spiking of sera with non-biotinylated ASARM-peptide was also carried out to determine recovery.

Immunohistochemistry of renal sections using anti-ASARM-peptide polyclonals

Mice (three hyp male mice and three normal male littermates) were first anesthetized with metofane and cardiac exsanguination was used to remove blood for serum preparation using humane methods and protocols approved by IACUC and UTHSCSA. After exsanguination, left kidneys were then removed from mice and immediately preserved in Millonig's phosphate buffered formalin (MPBF; Medical Industries Inc.). The collected and processed mice sera were used for ELISA analysis as described above. For immunohistochemical detection of ASARM-peptide epitopes, 3 µm thin sections prepared from paraffin-embedded kidneys were incubated with polyclonal anti-ASARM-peptide antibodies raised against the same MEPE C-terminal ASARM-peptide used for ELISA analysis (see above). The immunological reaction was visualized by an ABC alkaline phosphatase kit (Vector) and counter-stained with Mayer's hematoxylin–eosin (Fig. 3). The effects of blocking the renal immuno-positive reactions were investigated by spiking the anti-ASARM-peptide polyclonal antibodies with excess ASARM-peptide (250 µM). Additional control renal sections were also screened with pre-immune antisera derived from the same animals used to raise the anti-ASARM-peptide polyclonals.

Statistical analysis

Differences were assessed statistically by the use of Newman-Keuls, Bonferroni multiple comparison equations after one-way analysis of variance (non-parametric)

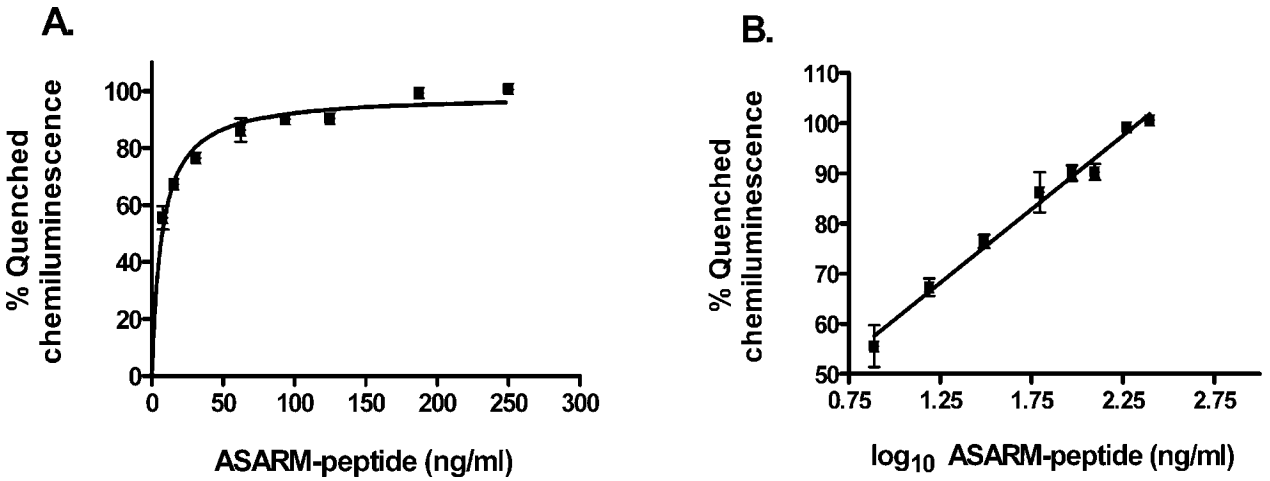

Figure 1 Competitive ELISA plots of percentage-quenching (y-axis) against non-biotinylated peptide (x-axis). Anti-ASARM-peptide polyclonal was first bound onto protein-G 96-micro-well plates. A constant concentration of biotinylated-ASARM-peptide (0·5 ng/ml) was then separately mixed with different concentrations of non-biotinylated ASARM-peptide and then added to the plates. The relative degree of chemiluminescent quenching was then assayed after addition of streptavidin–horseradish–peroxidase conjugate and measurement of light emission by a Bio-Rad FlourImager max system as described in Material and Methods. Graph A: Illustrates percentage-quenching data directly plotted against ASARM-peptide (ng/ml) (K_D of 7·5 ng/ml and a Q_{max} (quench maximum) of 98·7%). Graph B: Illustrates the same data but with a $\log_{10}$ ASARM-peptide (ng/ml) transform on the X-axis. A linear regression confirms a significant linear-regression fit (r^2=0·9405, P<0·0001) and the linear range for ASARM-peptide assay was 10 to 200 ng/ml (4·8 to 95·2 nM). Spiking of serum samples with non-biotinylated ASARM-peptide confirmed a greater than 87% recovery of product.

or *t*-tests (as indicated). A *P* value of less than 0·05 was considered significant. The standard error of the mean (S.E.M.) was used as a representative measure of how far the sample mean differed from the true population mean. Quantity 1 Bio-Rad software was used to analyze the intensity of chemiluminescent light-emission of samples and this was captured by a Bio-Rad FluorMax digital imaging system and data incorporated into GraphPad Prizm-4 software (Graphpad software. Inc.), for statistical analysis.

Results

Competitive ELISA using biotinylated and non-biotinylated ASARM-peptides

A competitive ELISA method was used to measure the levels of ASARM-peptide epitopes in serum as described in methods. Fig. 1A and B show the results derived from standard competition experiments (6 experiments, each sample in triplicate) containing 0·5 ng/ml biotinylated peptide and increasing concentrations of non-biotinylated synthetic ASARM-peptide. In Fig. 1A, a one site binding hyperbola clearly demonstrates a classic increased quenching of chemiluminescence correlated with increasing amounts of non-biotinylated ASARM-peptide in the presence of a constant amount (0·5 ng/ml) of biotinylated peptide. A K_D of 7·5 ng/ml and a Q_{max} (quench maximum) of 98·7% was obtained. A plot of $\log_{10}$ transformation of concentrations against percent quenching (Fig. 1B) enabled a linear regression curve to be computed (P<0·0001 and r^2=0·9405). The linear range for ASARM-peptide assay was 10–200 ng/ml (4·8 to 95·2 nM). Spiking of serum samples with non-biotinylated ASARM-peptide confirmed a greater than 87% recovery of product.

Serum ASARM-peptides in human and mouse X-linked rickets (HYP/hyp)

Figure 2 graphically depicts $\log_{10}$ dilution-transformation linear regression results as an end-point histogram for both HYP patients and hyp mice. The levels of ASARM-peptide epitope are elevated 5 fold in human subjects affected with HYP (P=0·007) relative to normal subjects (3·25 μM normal; 15·74 μM HYP). The levels of ASARM-peptide are also dramatically elevated in hyp-mice but even more so with a 6·2 fold increase compared with normal male siblings (3·73 μM and 23·4 μM).

ASARM-peptide epitope elevated binding in hyp renal proximal convoluted tubules

Figure 3 shows a cross section of hyp mice and normal littermates renal cortex paraffin sections screened with MEPE anti-ASARM polyclonal antibodies. Immuno-positive staining was markedly more pronounced in the hyp renal sections relative to normals. Moreover the staining was localized to areas anatomically consistent with the proximal convoluted tubules. The glomeruli are also clearly visible in all sections but were not immuno-positive. The ASARM immuno-positive staining was

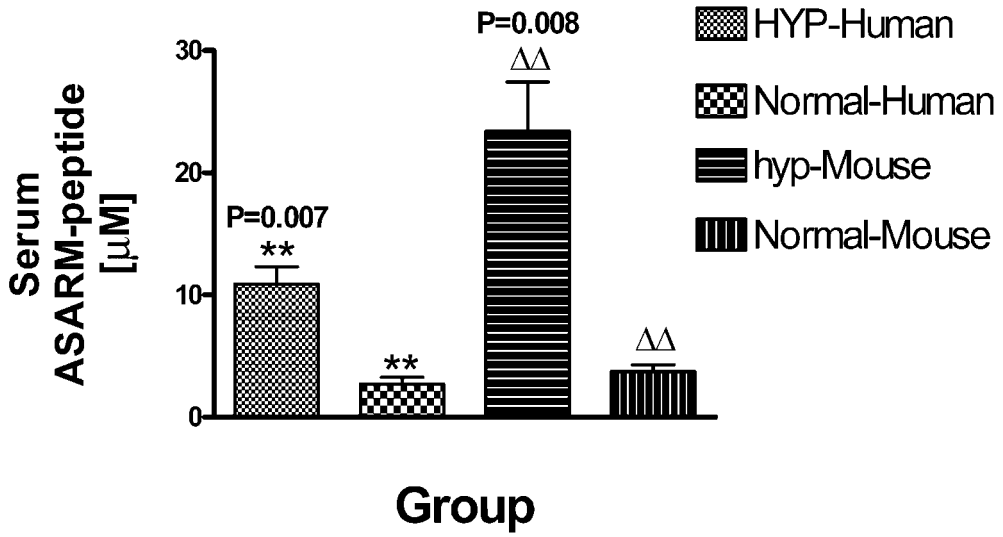

Figure 2 A histogram plot is presented that compares levels of ASARM-epitope(s) in normal human and mice sera relative to HYP/hyp counterparts. Concentrations of ASARM-peptide were calculated from the concentrations of peptide determined at three different dilutions of sera for each individual. A five-fold (P=0·007) increase in ASARM-epitopes were measured in HYP patients (n=9) relative to normal subjects (n=9). A six-fold increase (P=0·008) was measured in male hyp mice (n=3) compared with normal male siblings (n=3).

completely blocked with immunizing ASARM-peptide and pre-immune sera also gave a negative result (see Materials and Methods).

Discussion

This study confirms a marked elevation of serum ASARM-peptides in human subjects affected with X-linked hypophosphatemic rickets (HYP). Also, a similar elevation was observed in the murine homologue of X-linked rickets (hyp), specifically, in male hyp mice relative to their normal male littermates. Although the levels of ASARM-peptides were markedly elevated in both humans and mice affected with the disease the increase was greater in the hyp mice (5 fold in humans, 6·2 fold in mice). We speculate that this may be due to the fact that some of the human subjects were under treatment with calcitriol and phosphate supplements to counteract the disease. Calcitriol (1,25-vitamin D3) suppresses MEPE expression (Argiro *et al.* 2001, Okano *et al.* 2003, Rowe *et al.* 2004*b*) and thus may have indirectly contributed to a reduction in ASARM-peptide levels in the treated human patients.

The ASARM-motif is a potent inhibitor of mineralization and recombinant-MEPE is phosphaturic *in vitro* and *in vivo* (Rowe 2004, Rowe *et al.* 2004*a*, Rowe *et al.* 2004*b*). Also, the statherin ASARM-motif plays a key role in preventing the ectopic precipitation of calcium and phosphate salts in normal supersaturated saliva and is a potent inhibitor of mineralization (Long *et al.* 1998, Raj *et al.* 1992, Schwartz *et al.* 1992). Statherin is also thought to play a role in phosphate and calcium transport in the parotid glands and dentin mineralization dynamics. Remarkably this short salivary peptide maps to the same locality as MEPE on chromosome 4 in a region clustered with bone-dentin proteins (Rowe 2004, Rowe *et al.* 2004*b*). This group of proteins (osteopontin, DMP-1, BSP, DSPP, enamelin and MEPE) share many features and have been grouped in the SIBLING family (Fisher *et al.* 2001, Rowe 2004, Rowe *et al.* 2000). Osteopontin, DSPP, DMP-1 and MEPE also contain the ASARM-like motif and the fact that statherin maps to this region suggests an ancestral link between this important group of bone-dentin mineralization genes (Rowe 2004).

The ASARM-motif has distinct physicochemical and biological features that compare remarkably well with phosphonoformic acid (PFA) and also bisphosphonates (like etidronate). These molecules are small, highly charged, acidic with low pIs and phosphorylated. Both PFA and etidronate have dramatic effects on mineralization (inhibition) and renal phosphate, vitamin D metabolism and renal-phosphate uptake *in vivo* and *in vivo* (Loghman-Adham 1996, Loghman-Adham & Dousa 1992, Loghman-Adham *et al.* 1993, VanScoy *et al.* 1988). Also PFA and etidronate bind to the renal Na-phosphate co-transporter (NPT2) and effect an inhibition of phosphate uptake (Loghman-Adham 1996, Loghman-Adham & Dousa 1992, Loghman-Adham *et al.* 1993, VanScoy *et al.* 1988). In the case of PFA, dual effects

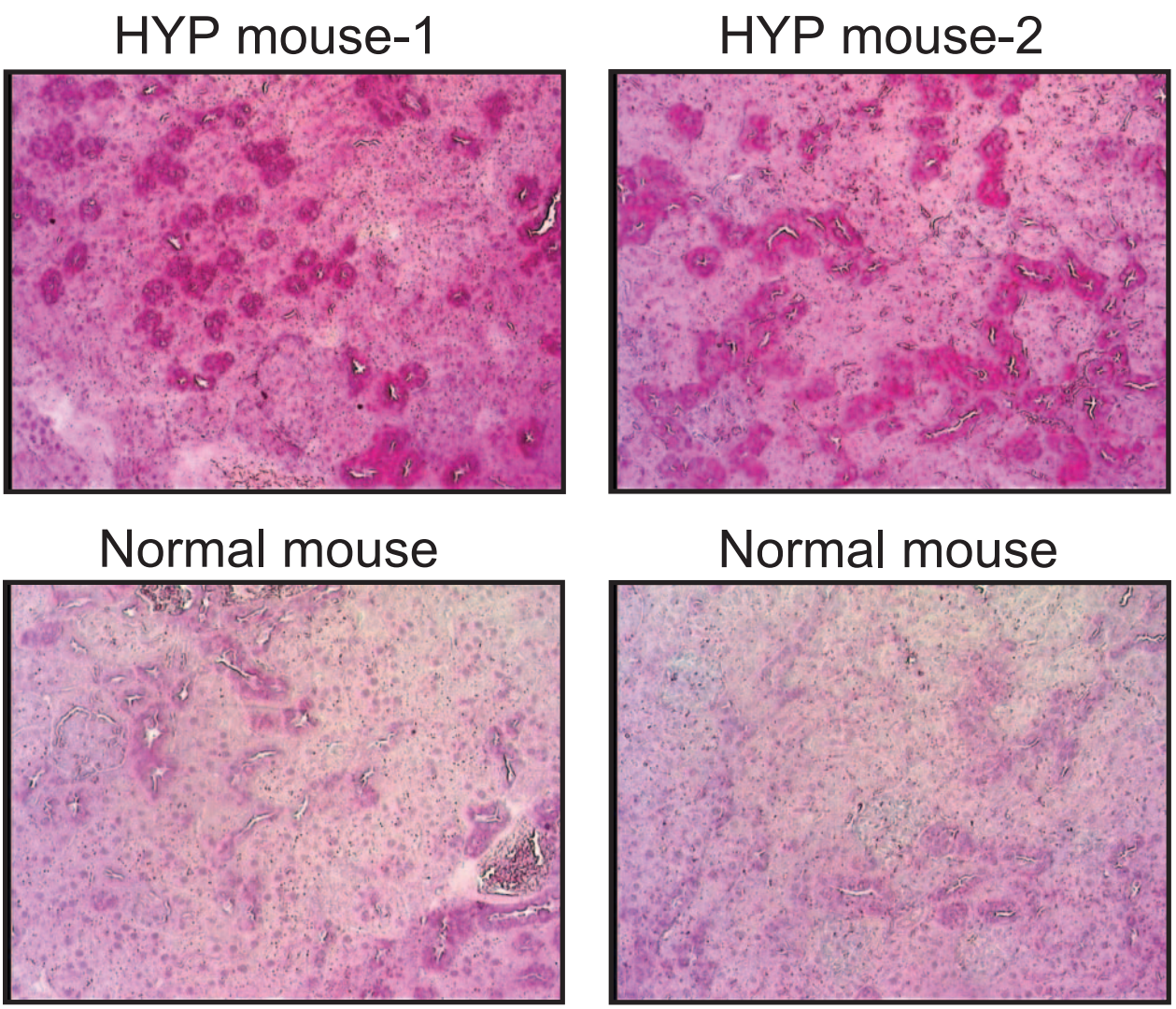

Figure 3 Immunohistochemical screen of hyp-mouse and normal-mouse renal cross-sections with anti-ASARM-peptide polyclonals. The expression of ASARM-peptide epitopes (bright red stain) was dramatically increased in male hyp-mice (upper two photographs) compared with normal male siblings mice at 8 weeks (lower two photographs). The ASARM-peptide staining is anatomically consistent with the renal proximal convoluted tubules. This region also stains positive for the sodium phosphate cotransporter type IIa (NaPi-2a). Nuclear-counterstaining was performed using standard hematoxylin and renal glomeruli are clearly visible in normal and hyp kidneys. Magnification: X10. The ASARM immuno-positive staining was completely blocked with immunizing ASARM-peptide and pre-immune sera also gave a negative result (see Materials and Methods).

on phosphate uptake have been demonstrated and are thought to be due to the reversible and specific binding of this molecule (PFA) to the renal phosphate co-transporter (Loghman-Adham & Dousa 1992). In brief, chronic exposure and thus binding of PFA to the NPT2 transporter likely results in an increase in mobilization and expression of NPT2, but, the saturated levels of PFA continue to sterically interfere with transport function with consequential inhibition of phosphate transport. This is confirmed by the fact that *in vitro*, if repeated washes are administered to attached renal cells previously exposed to PFA, a reversal of inhibition occurs and an increase of phosphate uptake ensues (Loghman-Adham & Dousa 1992).

In this study we have demonstrated that ASARM-peptides are not only elevated in HYP/hyp but also for the first time demonstrate accumulation in the renal proximal convoluted tubules of hyp mice. This is consistent with the known phosphaturic effects of rec-MEPE *in vivo* and *in vitro*. Moreover this is also consistent with the known biological effects of PFA/etidronate and the shared physicochemical features with the ASARM-peptide.

The MEPE ASARM-peptide is a known inhibitor of mineralization as are other ASARM-motifs in molecules such as statherin and osteopontin (Bennick *et al.* 1981, Hoyer *et al.* 2001, Long *et al.* 1998, Raj *et al.* 1992, Rowe 2004, Rowe *et al.* 2004*a*, Rowe *et al.* 2004*b*, Schlesinger & Hay 1977). Moreover, the levels measured in HYP patient and hyp mouse serum are commensurate with the levels that would cause phosphaturia and an inhibition of mineralization (Rowe *et al.* 2004*a*, Rowe *et al.* 2004*b*). Thus we conclude that the ASARM-peptide plays a major role in the pathophysiology of HYP/hyp. Moreover, since HYP pathophysiology overlaps with TIO and MEPE tumor-expression is a feature of this tumor-induced disease, we would expect a similar elevation of ASARM-peptides in TIO. Preliminary data on one of our TIO patients indicates that this is indeed the case. However, this needs to be confirmed by a detailed analysis of a number of patients with TIO before and after resection of tumors. Also, given that serum MEPE levels and expression show tight correlations and associations with serum PO_4, PTH, bone mineral density, serum 1,25 vitamin D3, PHEX and FGF-23 (Jain *et al.* 2004, Liu *et al.* 2003, Rowe *et al.* 2004*b*), a physiological role for MEPE in bone-mineral and renal-phosphate handling is likely.

A caveat must be included concerning the derivation of the ASARM-peptide(s) measured in these studies. Specifically, DMP-1, OPN, DSPP and statherin contain the ASARM-motif and likely share epitopes with the MEPE-ASARM-peptide. Thus we cannot exclude the possibility that our anti-ASARM-peptide polyclonals are wholly specific for the MEPE derived ASARM-motif. However, given that MEPE expression is markedly elevated in HYP and is tightly correlated with serum PO_4, PTH, BMD, 1,25 vitamin D3 and FGF23, the MEPE source of ASARM-peptide is likely predominant in serum. Also, our observations for the first time provide a compelling and novel link with the extracellular-matrix derived ASARM-peptide(s) and the dynamics of renal phosphate handling/bone-dental mineralization in disease and health.

Finally, we have recently demonstrated a specific non-proteolytic protein–protein association between MEPE and PHEX using surface plasmon resonance technology (Rowe *et al.* 2004*a*). Moreover, SPR peptide competition experiments confirm that the carboxy-terminal ASARM-motif plays a key role in this Zn-dependent interaction. N-terminal, mid-region RGD-MEPE peptides and control peptides were unable to inhibit the PHEX-MEPE interaction. Thus we conclude that PHEX may act by sequestering and protecting MEPE from proteolysis and thus preventing release of free protease-resistant ASARM-peptide. In HYP/hyp, defective PHEX, elevated proteases and increased expression of MEPE result in increased ASARM-peptide with deleterious consequences to mineralization of bone and renal phosphate handling. These experiments for the first time confirm that these peptides are indeed elevated in HYP/hyp and this in turn provides compelling evidence for the ASARM-model in disease and health (Rowe 2004, Rowe *et al.* 2004*a*, Rowe *et al.* 2004*b*).

Acknowledgements

We thank Mr Brandon Sehlke for his technical assistance with the renal immuno-histology slides. We are also indebted to the support provided by the following National Institutes of Health (NIH) grants to P S N R: 1R03DE015900–01 (National Institute of Dental & Craniofacial Research) and NIH grant RO-1 AR51598–01 (National Institute of Arthritis and Musculoskeletal Skin Diseases). We wish to acknowledge the help and support of the XLH Network http://www.xlhnetwork.org/ and in particular Dr Larry Winger (XLH group coordinator, England) and Dr Gerry Morrow (clinician, England). The views expressed in this material are those of the authors and do not reflect the official policy or position of the US Government, the Department of Defense, or the Department of the Air Force. The authors declare that there is no conflict of interest that could prejudice the impartiality of this scientific work.

References

Argiro L, Desbarats M, Glorieux FH & Ecarot B 2001 Mepe, the gene encoding a tumor-secreted protein in oncogenic hypophosphatemic osteomalacia, is expressed in bone. *Genomics* **74** 342–351.

Bai X, Miao D, Panda D, Grady S, McKee MD, Goltzman D & Karaplis AC (2002) Partial rescue of the hyp phenotype by osteoblast-targeted PHEX (phosphate-regulating gene with homologies to endopeptidases on the X chromosome) expression. *Molecular Endocrinology* **16** 2913–2925.

Bennick A, McLaughlin AC, Grey AA & Madapallimattam G 1981 The location and nature of calcium-binding sites in salivary acidic proline-rich phosphoproteins. *Journal of Biological Chemistry* **256** 4741–4746.

Cai Q, Hodgson SF, Kao PC, Lennon VA, KLee GG, Zinsmiester AR & Kumar R 1994 Brief report inhibition of renal phosphate transport by a tumor product in a patient with oncogenic osteomalacia. *New England Journal of Medicine* **330** 1645–1649.

De Beur SM, Finnegan RB, Vassiliadis J, Cook B, Barberio D, Estes S, Manavalan P, Petroziello J, Madden SL, Cho JY, Kumar R, Levine MA & Schiavi SC 2002 Tumors associated with oncogenic osteomalacia express genes important in bone and mineral metabolism. *Journal of Bone and Mineral Research* **17** 1102–1110.

Dobbie H, Shirley DG, Faria NJ, Rowe PSN, Slater JM & Unwin RJ 2003 Infusion of the bone-derived protein MEPE causes phosphaturia in rats (Abstract: American Society for Nephrology (ASN) meeting). *Journal of the American Society of Nephrology* **14** 468A.

Drezner MK 1990 Tumour-associated rickets and osteomalacia. In *Primer on Metabolic Bone Diseases and Disorders of Mineral Metabolism*, pp 184–188. Ed MJ Favus. American Socity for Bone and Mineral Research, Kelseyville, CA, USA.

Drezner MK 2003 Hypophosphatemic rickets. *Endocrine Development* **6** 126–155.

Fisher LW, Torchia DA, Fohr B, Young MF & Fedarko NS 2001 Flexible structures of SIBLING proteins, bone sialoprotein, and osteopontin. *Biochemical and Biophysical Research Communications* **280** 460–465.

Gowen LC, Petersen DN, Mansolf AL, Qi H, Stock JL, Tkalcevic GT, Simmons HA, Crawford DT, Chidsey-Frink KL, Ke HZ, McNeish JD & Brown TA 2003 Targeted disruption of the osteoblast/osteocyte factor 45 gene (OF45) results in increased bone formation and bone mass. *Journal of Biological Chemistry* **278** 1998–2007.

Guo R, Rowe PS, Liu S, Simpson LG, Xiao ZS & Quarles LD 2002 Inhibition of MEPE cleavage by Phex. *Biochemical and Biophysical Research Communications* **297** 38–45.

Hoyer JR, Asplin JR & Otvos L 2001 Phosphorylated osteopontin peptides suppress crystallization by inhibiting the growth of calcium oxalate crystals. *Kidney International* **60** 77–82.

HYP-consortium, Francis F, Hennig S, Korn B, Reinhardt R, de Jong D, Poustka A, Lehrach H, Rowe PSN, Goulding JN, Summerfield T, Mountford RC, Read AP, Popowska E, Pronicka E, Davies KE, O'Riordan JLH, Econs MJ, Nesbitt T, Drezner MK, Oudet C, Pannetier S, Hanauer A, Strom TM, Meindl A, Lorenz B, Cagnoli M, Mohnike KL, Murken J & Meitinger T 1995 A gene (PEX) with homologies to endopeptidases is mutated in patients with X-linked hypophosphatemic rickets. The HYP Consortium. *Nature Genetics* **11** 130–136.

Jain A, Fedarko NS, Collins MT, Gelman R, Ankrom MA, Tayback M & Fisher LW 2004 Serum levels of matrix extracellular phosphoglycoprotein (MEPE) in normal humans correlate with serum phosphorus, parathyroid hormone and bone mineral density. *Journal of Clinical Endocrinology and Metabolism* **89** 4158–4161.

Jonsson KB, Mannstadt M, Miyauchi A, Yang IM, Stein G, Ljunggren O & Juppner H 2001 Extracts from tumors causing oncogenic osteomalacia inhibit phosphate uptake in opossum kidney cells. *Journal of Endocrinology* **169** 613–620.

Lajeunesse D, Meyer RA Jr. & Hamel L 1996 Direct demonstration of a humorally-mediated inhibition of renal phosphate transport in the Hyp mouse. *Kidney International* **50** 1531–1538.

Liu S, Guo R, Simpson LG, Xiao ZS, Burnham CE & Quarles LD 2003 Regulation of FGF23 expression but not degradation by phex. *Journal of Biological Chemistry* **278** 37419–37426.

Loghman-Adham M 1996 Use of phosphonocarboxylic acids as inhibitors of sodium-phosphate cotransport. *General Pharmacology* **27** 305–312.

Loghman-Adham M & Dousa TP 1992 Dual action of phosphonoformic acid on Na(+)-phosphate cotransport in opossum kidney cells. *American Journal of Physiology* **263** F301–F310.

Loghman-Adham M, Levi M, Scherer SA, Motock GT & Totzke MT 1993 Phosphonoformic acid blunts adaptive response of renal and intestinal Pi transport. *American Journal of Physiology* **265** F756–F763.

Long JR, Dindot JL, Zebroski H, Kiihne S, Clark RH, Campbell AA, Stayton PS & Drobny GP 1998 A peptide that inhibits hydroxyapatite growth is in an extended conformation on the crystal surface. *PNAS* **95** 12083–12087.

Nampei A, Hashimoto J, Hayashida K, Tsuboi H, Shi K, Tsuji I, Miyashita H, Yamada T, Matsukawa N, Matsumoto M, Morimoto S, Ogihara T, Ochi T & Yoshikawa H 2004 Matrix extracellular phosphoglycoprotein (MEPE) is highly expressed in osteocytes in human bone. *Journal of Bone and Mineral Metabolism* **22** 176–184.

Nelson AE, Namkung HJ, Patava J, Wilkinson MR, Chang AM, Reddel RR, Robinson BG & Mason RS 1996 Characteristics of tumor cell bioactivity in oncogenic osteomalacia. *Molecular And Cellular Endocrinology* **124** 17–23.

Nelson AE, Robinson BG, Hogan JJ, Dwight T & Mason RS 1997 Mechanism of inhibition of renal phosphate uptake by a tumor-derived factor in oncogenic osteomalacia (Abstract: American Society for Bone Mineral Research (ASBMR) meeting). *Journal of Bone and Mineral Research* **12** F679.

Nelson AE, Hogan JJ, Holm IA, Robinson BG & Mason RS 2001 Phosphate wasting in oncogenic osteomalacia PHEX is normal and the tumor-derived factor has unique properties. *Bone* **28** 430–439.

Nesbitt T, Fujiwara I, Thomas R, Xiao ZS, Quarles LD & Drezner MK 1999 Coordinated maturational regulation of PHEX and renal phosphate transport inhibitory activity evidence for the pathophysiological role of PHEX in X-linked hypophosphatemia. *Journal of Bone and Mineral Research* **14** 2027–2035.

Okano T, Tsugawa N, Hirami C & Kato S 2003 Functional properties of cultured normal and vitamin D receptor knockout mice calvarial osteoblasts (Abstract). *Journal of Bone and Mineral Research* **18** (Suppl 2) S141.

Petersen DN, Tkalcevic GT, Mansolf AL, Rivera-Gonzalez R & Brown TA 2000 Identification of osteoblast/osteocyte factor 45 (OF45), a bone-specific cDNA encoding an RGD-containing protein that is highly expressed in osteoblasts and osteocytes. *Journal of Biological Chemistry* **275** 36172–36180.

Quarles LD & Drezner MK 2001 Pathophysiology of X-linked hypophosphatemia, tumor-induced osteomalacia, and autosomal dominant hypophosphatemia a perPHEXing problem. *Journal of Clinical Endocrinology and Metabolism* **86** 494–496.

Raj PA, Johnsson M, Levine MJ & Nancollas GH 1992 Salivary statherin. Dependence on sequence, charge, hydrogen bonding potency, and helical conformation for adsorption to hydroxyapatite and inhibition of mineralization. *Journal of Biological Chemistry* **267** 5968–5976.

Rowe PSN 1998 The role of the PHEX gene (PEX), in families with X-linked hypophosphataemic rickets. *Current Opinion in Nephrology and Hypertension* **7** 367–376.

Rowe PSN 2004 The wrickkened-pathways of FGF23, MEPE and PHEX. *Critical Reviews in Oral Biology and Medicine* **15** 264–281.

Rowe PSN, Goulding J, Read A, Lehrach H, Francis F, Hanauer A, Oudet C, Biancalana V, Kooh SW, Davies KE & Oriordan JLH 1994 Refining the genetic-map for the region flanking the X-linked hypophosphatemic rickets locus (Xp22·1–22·2). *Human Genetics* **93** 291–294.

Rowe PSN, Goulding JN, Francis F, Oudet C, Econs MJ, Hanauer A, Lehrach H, Read AP, Mountford RC, Summerfield T, Weissenbach J, Fraser W, Drezner MK, Davies KE & Oriordan JLH 1996 The gene for X-linked hypophosphataemic rickets maps to a 200–300 kb region in Xp22·1, and is located on a single YAC containing a putative vitamin D response element (VDRE). *Human Genetics* **97** 345–352.

Rowe PSN, Oudet C, Francis F, Sinding C, Pannetier S, Econs MJ, Strom TM, Meitinger T, Garabedian M, David A, Macher M-A, Questiaux E, Popowska E, Pronicka E, Read AP, Mokrzycki A, Glorieux FH, Drezner MK, Hanauer A, Lehrach H, Goulding J & O'Riordan JLH 1997 Distribution of mutations in the PEX gene in families with X-linked hypophosphataemic rickets (HYP). *Human Molecular Genetics* **6** 539–549.

Rowe PSN, de Zoysa P, Dong R, Wang H, White K, Econs M & Oudet C 2000 MEPE, a new gene expressed in bone-marrow and tumours causing osteomalacia. *Genomics* **67** 54–68.

Rowe PSN, Garrett IR, Schwarz PM, Carnes DL, Lafer EM, Mundy GR & Gutierrez GE 2004*a* Surface Plasmon Resonance (SPR) confirms MEPE binds to PHEX via the MEPE-ASARM-motif A model for impaired mineralization in X-linked rickets (HYP). *Bone* (In Press).

Rowe PSN, Kumagai Y, Gutierrez G, Garrett IR, Blacher R, Rosen D, Cundy J, Navvab S, Chen D, Drezner MK, Quarles LD & Mundy GR 2004*b* MEPE has the properties of an osteoblastic phosphatonin and minhibin. *Bone* **34** 303–319.

Schlesinger DH & Hay DI 1977 Complete covalent structure of statherin, a tyrosine-rich acidic peptide which inhibits calcium phosphate precipitation from human parotid saliva. *Journal of Biological Chemistry* **252** 1689–1695.

Schwartz SS, Hay DI & Schluckebier SK 1992 Inhibition of calcium phosphate precipitation by human salivary statherin structure-activity relationships. *Calcified Tissue International* **50** 511–517.

Seufert J, Ebert K, Muller J, Eulert J, Hendrich C, Werner E, Schuuze N, Schulz G, Kenn W, Richtmann H, Palitzsch KD & Jakob F 2001 Octreotide therapy for tumor-induced osteomalacia. *New England Journal of Medicine* **345** 1883–1888.

Shimada T, Mizutani S, Muto T, Yoneya T, Hino R, Takeda S, Takeuchi Y, Fujita T, Fukumoto S & Yamashita T 2001 Cloning and characterization of FGF23 as a causative factor of tumor-induced osteomalacia. *PNAS* **98** 6500–6505.

Siggelkow H, Schmidt E, Hennies B & Hufner M 2004 Evidence of downregulation of matrix extracellular phosphoglycoprotein during terminal differentiation in human osteoblasts. *Bone* **35** 570–576.

Strom TM, Francis F, Lorenz B, Boddrich A, Econs MJ, Lehrach H & Meitinger T 1997 Pex gene deletions in Gy and Hyp mice provide mouse models for X-linked hypophosphataemia. *Human Molecular Genetics* **6** 165–171.

VanScoy M, Loghman-Adham M, Onsgard M, Szczepanska-Konkel M, Homma S, Knox FG & Dousa TP 1988 Mechanism of phosphaturia elicited by administration of phosphonoformate *in vivo*. *American Journal of Physiology* **255** F984–F994.

Wilkins GE, Granleese S, Hegele RG, Holden J, Anderson DW & Bondy GP 1995 Oncogenic osteomalacia evidence for a humoral phosphaturic factor. *Journal of Clinical Endocrinology and Metabolism* **80** 1628–1634.

Xiao ZS, Crenshaw M, Guo R, Nesbitt T, Drezner MK & Quarles LD 1998 Intrinsic mineralization defect in Hyp mouse osteoblasts. *American Journal of Physiology* **275** E700–E708.